

## NEUROSCIENCE

# Design of fast-onset antidepressant by dissociating SERT from nNOS in the DRN

Nan Sun<sup>1,2†</sup>, Ya-Juan Qin<sup>3†</sup>, Chu Xu<sup>1,4†</sup>, Tian Xia<sup>1†</sup>, Zi-Wei Du<sup>1</sup>, Li-Ping Zheng<sup>3</sup>, An-an Li<sup>5</sup>, Fan Meng<sup>1</sup>, Yu Zhang<sup>1</sup>, Jing Zhang<sup>1</sup>, Xiao Liu<sup>6</sup>, Ting-You Li<sup>3,\*</sup>, Dong-Ya Zhu<sup>1,7\*</sup>, Qi-Gang Zhou<sup>1,7,8\*</sup>

Major depressive disorder (MDD) is one of the most common mental disorders. We designed a fast-onset antidepressant that works by disrupting the interaction between the serotonin transporter (SERT) and neuronal nitric oxide synthase (nNOS) in the dorsal raphe nucleus (DRN). Chronic unpredictable mild stress (CMS) selectively increased the SERT-nNOS complex in the DRN in mice. Augmentation of SERT-nNOS interactions in the DRN caused a depression-like phenotype and accounted for the CMS-induced depressive behaviors. Disrupting the SERT-nNOS interaction produced a fast-onset antidepressant effect by enhancing serotonin signaling in forebrain circuits. We discovered a small-molecule compound, ZZL-7, that elicited an antidepressant effect 2 hours after treatment without undesirable side effects. This compound, or analogous reagents, may serve as a new, rapidly acting treatment for MDD.

**M**ajor depressive disorder (MDD) is one of the most common mental disorders (1). The serotonin transporter (SERT) is presently the primary target for antidepressants (2). However, SERT inhibitors have serious limitations: (i) they take at least 3 to 4 weeks to take effect, (ii) only a portion of patients recover after treatment, and (iii) they have extensive side effects, including suicide in some patients (3–5). Rapid elicitation of an antidepressant response by ketamine has been reported (6, 7). A low dose of ketamine effectively inhibited the suicidal tendency of patients and was effective in >70% of patients with refractory depression within hours of administration (8, 9). However, potential addictive properties and the risk for schizophrenia have raised concerns. Therefore, scientists are still searching for new, fast-acting antidepressant targets and compounds (10–13).

The dorsal raphe nucleus (DRN) is a main source of 5-hydroxytryptamine (5-HT) in the

brain. It projects to the cortex and limbic system and plays a major role in modulating depressive mood (14, 15). The effect of the 5-HT/5-HT<sub>1A</sub> autoreceptor (5-HT<sub>1A</sub>R<sub>auto</sub>) in the DRN is completely opposite to that of 5-HT/postsynaptic 5-HT<sub>1A</sub> heteroreceptor (5-HT<sub>1A</sub>R<sub>heter</sub>) in the cortex and hippocampus (HPC) (14, 16, 17). Under physiological conditions, the activation of somatodendritic 5-HT<sub>1A</sub>R<sub>auto</sub> in the DRN represses neural firing of serotonergic neurons, leading to decreased 5-HT release in the cortex, HPC, and other parts of the brain (14). Under depressive status, somatodendritic 5-HT<sub>1A</sub>R<sub>auto</sub>s in the DRN are hyperactive, causing a reduced firing frequency of 5-HT neurons, a low 5-HT level in the synaptic cleft, and deactivation of postsynaptic 5-HT<sub>1A</sub>R<sub>heter</sub>s (18, 19). SERT inhibitors activate both somatodendritic 5-HT<sub>1A</sub>R<sub>auto</sub>s and postsynaptic 5-HT<sub>1A</sub>R<sub>heter</sub>s. Desensitization of 5-HT<sub>1A</sub>R<sub>auto</sub>s breaks the balance between 5-HT<sub>1A</sub>R<sub>auto</sub>s and 5-HT<sub>1A</sub>R<sub>heter</sub>s within weeks after treatment and induces antidepressant effects through postsynaptic 5-HT<sub>1A</sub>R<sub>heter</sub>s (14, 20, 21), indicating that enhanced DRN 5-HT/5-HT<sub>1A</sub>R<sub>auto</sub> signaling is the primary reason for the delayed onset of SERT inhibitors.

Neuronal nitric oxide synthase (nNOS) controls the cell surface localization of SERT through physical interaction between nNOS and SERT in the DRN (22). The cell surface localization of SERT determines the intercellular 5-HT concentration in the DRN and thus the function of DRN 5-HT<sub>1A</sub>R<sub>auto</sub>s (2). We hypothesized that dissociating SERT from nNOS may diminish DRN 5-HT/5-HT<sub>1A</sub>R<sub>auto</sub> signaling by enhancing SERT function, thereby enhancing the firing of DRN serotonergic neurons. If this is indeed the case, then SERT-nNOS interaction blockers (SNIBs) may produce a fast-onset antidepressant effect without the drawbacks of current monoamine antidepressants.

## Results

## DRN SERT-nNOS coupling is implicated in the modulation of depressive behaviors

SERT interacts with nNOS through the binding of its C-tail motif to the atypical disk large/ZO-1 (PDZ) domain of nNOS in the DRN (22). We observed ~90% co-localization of nNOS and SERT immunoreactivities in the mouse DRN (fig. S1A). Coimmunoprecipitation and Western blot revealed that the levels of SERT, the SERT-nNOS complex, and the complex as fraction of total SERT protein in the DRN were much higher than in other depression-associated brain regions, including the HPC, prefrontal cortex (PFC), nucleus accumbens, hypothalamus, and corpus striatum, suggesting a selective enrichment of the complex as a fraction of total SERT protein in the DRN (fig. S1B). The selective enrichment of SERT-nNOS complex is possibly due to the lack of nNOS in the presynaptic part in the terminal regions of serotonergic neurons such as those in the PFC and HPC (fig. S1C). CMS is a classic model of depression in rodents. Four-week CMS exposure caused a significantly increased SERT-nNOS complex in the DRN of mice but not in other brain regions (fig. S1, D and E). However, CMS did not affect mRNA and protein levels of nNOS, nitric oxide production, and protein nitrosylation in the DRN (fig. S1, F to I).

To selectively disrupt the SERT-nNOS interaction in DRN serotonergic neurons, we conditionally knocked out *nNos* in TPH2-positive neurons (Fig. 1A). In *Tph2-CreER; nNos<sup>loxP/loxP</sup>* mice, no nNOS was detected in the DRN serotonergic neurons (Fig. 1B and fig. S1J), and the nNOS level in the DRN was much lower than that in *nNos<sup>loxP/loxP</sup>* mice (Fig. 1C). *Tph2-CreER; nNos<sup>loxP/loxP</sup>* mice showed significantly increased SERT on the cell membrane surface in the DRN (Fig. 1C and fig. S1, K and L) and displayed antidepressant-like behaviors as shown by the tail suspension test (TST) and forced swimming test (FST) 4 weeks after tamoxifen administration (Fig. 1D). No abnormal phenotype was observed in *nNos<sup>loxP/loxP</sup>* mice compared with wild-type (WT) mice (fig. S1, M to P).

To further examine the role of SERT-nNOS coupling in the DRN as it relates to depression, we screened our compound library previously established on the basis of nNOS-mediated protein-protein interactions, some of which has been published previously (23–26). Unexpectedly, we found that two compounds of the Sakura series (fig. S2A), Sakura-6 (*N*-cyclohexylethyl-Ala-Asp-Trp-Val-OH) and Sakura-8 (*N*-cyclohexylethyl-Ala-Asp-Ala-Val-OH), significantly increased the SERT-nNOS complex but decreased the cell surface SERT level, thus working as SERT-nNOS interaction promoters (Fig. 1, E and F, and fig. S2, B and C). Microinjection of Sakura-6 into the DRN acutely (2 hours after injection) caused depression-like behaviors in mice, as indicated by enhanced

<sup>1</sup>State Key Laboratory of Reproductive Medicine, Department of Clinic Pharmacology, School of Pharmacy, Nanjing Medical University, Nanjing 211166, China. <sup>2</sup>Jiangsu Province Key Laboratory of Anesthesiology, Jiangsu Province Key Laboratory of Anesthesia and Analgesia Application, NMPA Key Laboratory for Research and Evaluation of Narcotic and Psychotropic Drugs, Xuzhou Medical University, Xuzhou 221004, China. <sup>3</sup>Department of Pharmacochimistry, School of Pharmacy, Nanjing Medical University, Nanjing 211166, China. <sup>4</sup>Institute of Dermatology, Chinese Academy of Medical Science and Peking Union Medical College, Nanjing 210042, China. <sup>5</sup>Jiangsu Key Laboratory of Brain Disease and Bioinformation, Research Center for Biochemistry and Molecular Biology, Xuzhou Medical University, Xu Zhou 221004, China. <sup>6</sup>College of Pharmacy, Nanjing University of Chinese Medicine, Nanjing 210023, China. <sup>7</sup>The Key Center of Gene Technology Drugs of Jiangsu Province, Nanjing Medical University, Nanjing 211166, China. <sup>8</sup>Department of Clinic Pharmacology, Sir runrun Hospital, Nanjing Medical University, Nanjing 211167, China.

\*Corresponding author. Email: dyzhu@njmu.edu.cn (D.-Y.Z.); l.tingyou@njmu.edu.cn (T.-Y.L.); qigangzhou@njmu.edu.cn (Q.-G.Z.)

†These authors contributed equally to this work.

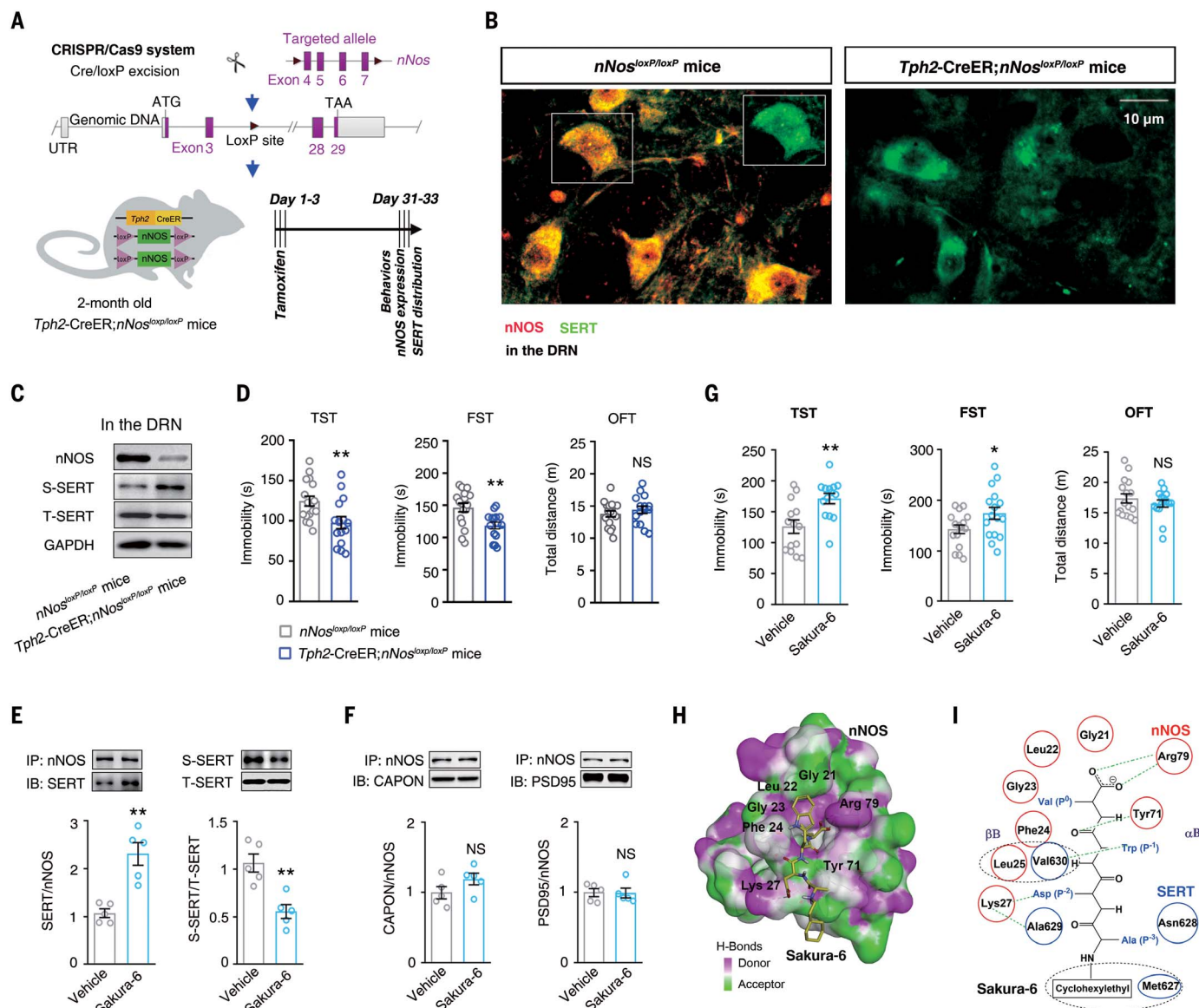


**Fig. 1. Depression-like phenotype induced by promoting the level of SERT-nNOS coupling in the DRN.** (A) Schematic of construction of *nNos<sup>loxP/loxP</sup>* mice using the CRISPR-Cas9 technique. (B) Expression level of SERT and nNOS in serotonergic neurons 1 min after conditional knockout of *nNos* as shown by immunofluorescence ( $n = 5$  mice). (C) Expression of nNOS and SERT in the DRN after conditional deletion of nNOS in the serotonergic neurons ( $n = 5$  mice). (D) Animal behavior in the TST, FST, and open-field test (OFT) 1 min after tamoxifen administration ( $n = 15$  to 18 mice; data were analyzed with Student's *t* test). (E) SERT-nNOS coupling level and membrane expression of SERT in the DRN 2 hours after infusion of Sakura (3  $\mu$ g, 200 nl) into the DRN ( $n = 5$  mice; data were analyzed with Student's *t* test). (F) nNOS-CAPON and nNOS-PSD95 coupling level and membrane expression of SERT in

the DRN 2 hours after infusion of Sakura (1  $\mu$ g) into the DRN ( $n = 5$  mice; data were analyzed with Student's *t* test). (G) Depression-related behavior change measured by the FST, TST, and OFT 2 hours after infusion of Sakura (1  $\mu$ g) into the DRN ( $n = 14$  to 16 mice; data were analyzed with Student's *t* test). (H) Soft hydrogen bond donor/acceptor surface of the binding pocket of nNOS PDZ with Sakura. (I) Proposed interactions among SERT, Sakura-6, and the nNOS PDZ domain. Val<sup>630</sup>, Ala<sup>629</sup>, Asn<sup>628</sup>, and Met<sup>627</sup> are the C-terminal tetrapeptide of SERT. Gly<sup>21</sup>, Leu<sup>22</sup>, Gly<sup>23</sup>, Phe<sup>24</sup>, Lys<sup>27</sup>, Tyr<sup>71</sup>, and Arg<sup>79</sup> are part of nNOS PDZ domain. \* $P < 0.05$ ; \*\* $P < 0.01$ ; NS, not significant. Error bars indicate SEM. S-SERT, cell membrane surface SERT; T-SERT, total SERT of the whole cell; IB, immunoblotting; IP, immunoprecipitation; Co-IP, coimmunoprecipitation analysis; WB, Western blot analysis.

immobility time in the TST and FST (Fig. 1G). This treatment did not change the total content of nNOS and SERT (fig. S2D) and had no impact on nNOS-C-terminal PDZ ligand of nNOS (CAPON) coupling and nNOS-postsynaptic density protein-95 (PSD95) coupling in the DRN (Fig. 1F). Pretreatment with intra-DRN Way-100635, a 5-HT<sub>1A</sub>R antagonist, blocked

the effect of Sakura-6 (fig. S2E), implicating the DRN 5-HT<sub>1A</sub>R in the effect. In addition, microinjecting Sakura-6 into the medial PFC (mPFC) or the ventral HPC (vHPC), the two brain regions that receive serotonergic projections and are closely related to depression (27, 28), did not induce depression-like behavior (fig. S2, F and G), and microinjection of

Sakura-8 into the DRN, the other screened SERT-nNOS interaction promotor, also induced depression-like behavior (fig. S2H), further confirming an important role of DRN SERT-nNOS in the modulation of depression. Through molecular docking and chemical calculations, we speculated that Sakura may act as linker between the nNOS PDZ domain and SERT to

facilitate the association of nNOS and SERT (Fig. 1, H and I).

Next, we constructed a recombinant lentiviral vector carrying full-length cDNA of nNOS with or without a mutated nucleotide critical for the catalytic activity (29) (LV-nNOS-GFP and LV-nNOSA-GFP) (fig. S3, A and B). We infused LV-nNOS-GFP, LV-nNOSA-GFP, or LV-GFP into the DRN of mice. Overexpression of nNOSA lacking catalytic activity resulted in a significantly increased SERT-nNOSA complex and a decreased cell surface SERT level (fig. S3, C and D), and caused depression-like behaviors, as shown by TST and FST, 28 d after virus infection (fig. S3E). However, overexpression of nNOS did not have this effect (fig. S3, F and G), possibly because of the unexpected effects of forced overproduction of nitric oxide (22).

### **Dissociating SERT from nNOS in the DRN produces a fast-onset antidepressant effect**

Serotonergic neuronal activity is essential for the regulation of emotion and DRN somatodendritic 5-HT<sub>1A</sub>R<sub>auto</sub>s, which is crucial for the self-inhibitory mechanism of serotonergic neuronal activity (14, 30). A PDZ-binding motif of nNOS, the 15 C-terminal amino acids (TPTEIPCGDIRMNAV) of SERT (SERT-15C), is sufficient for the interaction between SERT and nNOS, and the SERT-nNOS association diminishes the cell surface localization of SERT in the brain and thereby reduces 5-HT reuptake of serotonergic neurons in the DRN (22). On the basis of these previous results and our present data (Fig. 1), we hypothesized that emotional stress may reduce the cell surface localization of SERT by promoting a SERT-nNOS association, thereby facilitating the activation of DRN 5-HT<sub>1A</sub>R<sub>auto</sub>s and causing depression. Therefore, dissociating SERT from nNOS may reverse this pathological process (Fig. 2A). We synthesized a peptide named Tat-SERT-15C, in which the SERT-15C was N-terminally fused to the transduction domain of the Tat protein from the HIV type 1 (YGRKKRRQRRR) to permit its intracellular delivery. We incubated the 293T cell line transfected by the full length of cDNA encoding SERT and nNOS with Tat-SERT-15C and found that Tat-SERT-15C decreased the SERT-nNOS complex and increased SERT in the cell surface dose dependently (fig. S4A). Microinjection of Tat-SERT-15C into the DRN of mice caused a reduction in the SERT-nNOS complex as a fraction of total SERT protein, a significant increase in the SERT level in the cell surface 2 hours after the microinjection (fig. S4B), and a significant decrease in the intercellular 5-HT concentration in the DRN measured in vivo (fig. S4C), and produced an antidepressant-like effect (fig. S4D). Moreover, the treatment did not change nNOS-PSD95 and nNOS-CAPON complex levels in the DRN (fig. S4E). Microinjection of a modified peptide with 15 ran-

dom amino acids (KKADNHSMGAYAGHK) fused to Tat (Tat-Control-15A), which is not capable of disrupting the SERT-nNOS interaction, into the DRN did not cause a depression-like behavior change (fig. S4F). Additionally, microinjecting Tat-SERT-15C into the DRN of *nNos*<sup>-/-</sup> mice did not affect depression-related behaviors (fig. S4G).

Next, we microinjected Tat-SERT-15C, fluoxetine, or vehicle into the DRN of mice at 29 d after CMS exposure for 28 d (28d-CMS). We measured SERT expression, SERT-nNOS complex and intercellular 5-HT in the DRN, and depression behaviors using the TST, FST, and sucrose preference test 2 hours after microinjection. CMS significantly increased the intercellular 5-HT concentration (Fig. 2B) and SERT-nNOS complex and decreased the cell surface SERT level in the DRN (Fig. 2C). Tat-SERT-15C reversed the CMS-induced changes (Fig. 2, B and C). However, fluoxetine, a classical SERT inhibitor, amplified the CMS-induced elevation in intercellular 5-HT in the DRN (Fig. 2B). CMS-caused depression behaviors were reversed by Tat-SERT-15C acutely (Fig. 2D). Systematic treatment of Tat-SERT-15C in mice subjected to 28d-CMS produced similar effects (fig. S4, H and I). Moreover, we microinjected 8-OH-DPAT, a selective agonist of 5-HT<sub>1A</sub>R, into the DRN through a previously implanted cannula and then administered mice with Tat-SERT-15C intraperitoneally. Behavior tests 2 hours after treatment showed that 8-OH-DPAT significantly blocked the induction of antidepressant-like behaviors by Tat-SERT-15C (Fig. 2E). Moreover, activating DRN somatodendritic 5-HT<sub>1A</sub>R<sub>auto</sub>s by 8-OH-DPAT or deactivating 5-HT<sub>1A</sub>R<sub>auto</sub>s by Way-100635 was sufficient to induce a depression-like or an antidepressant-like effect (Fig. 2, F and G). Together, these data suggest that the SERT-nNOS interaction modulates depression through DRN somatodendritic 5-HT<sub>1A</sub>R<sub>auto</sub>s (Fig. 2A).

### **Activating the serotonergic circuit is crucial for the action of SERT-nNOS in the DRN**

The activity of DRN serotonergic neurons is regulated by negative feedback from intercellular 5-HT acting through somatodendritic 5-HT<sub>1A</sub>R<sub>auto</sub>s (16, 31). We thus investigated whether the fast-onset antidepressant effect of Tat-SERT-15C was due to the enhancement of firing activity of DRN serotonergic neurons (Fig. 3A). To test this, we optogenetically stimulated DRN neurons and recorded neural firing 28 d after AAV infection (Fig. 3, B and C). Tat-SERT-15C was given 2 hours before in vivo electrophysiology recording (Fig. 3B). Tat-SERT-15C increased the neural firing rate of serotonergic neurons significantly compared with vehicle (Fig. 3C). To determine whether the enhanced firing activity of serotonergic neurons is necessary for the effect of Tat-SERT-15C on behaviors, we silenced DRN neu-

rons expressing SERT in the presence of the designer receptors exclusively activated by designer drugs (DREADDs) agonist clozapine-N-oxide (CNO) (Fig. 3D). Four weeks after AAV infection, we injected Tat-SERT-15C or vehicle with or without CNO to these mice 2 hours before performing behavioral tests. Although the mice treated with Tat-SERT-15C without CNO displayed marked antidepressant-like behaviors, the mice treated with Tat-SERT-15C plus CNO did not (Fig. 3E). Moreover, these treatments did not affect locomotor activity of mice in the open-field test (Fig. 3E).

Terminal serotonin release into the mPFC and vHPC is strictly controlled by firing activity of serotonergic neurons in the DRN, and the firing activity is negatively regulated by DRN 5-HT<sub>1A</sub>R<sub>auto</sub>s (14). We thus hypothesized that the CMS-induced increase in intercellular 5-HT in the DRN (Fig. 2B) may activate 5-HT<sub>1A</sub>R<sub>auto</sub>s and weaken the activity of serotonergic neurons, resulting in reduced 5-HT release into the mPFC and vHPC. If this is the case, then dissociating SERT-nNOS may reverse the CMS-induced changes (Fig. 3A). We therefore measured concentrations of 5-HT in the DRN, mPFC, and vHPC 24 hours after microinjection of Tat-SERT-15C and fluoxetine into the DRN. Tat-SERT-15C decreased intercellular 5-HT in the DRN and increased intercellular 5-HT in the mPFC and vHPC significantly, whereas fluoxetine had the completely opposite effect (fig. S5, A and B). Although chronic administration of fluoxetine has antidepressant activity, acute microinjection of fluoxetine into the DRN induced depressive-like behavior (fig. S5C). Neither treatment affected intercellular NA and DA concentrations in any of the regions (fig. S5D). 28d-CMS exposure caused significantly reduced intercellular 5-HT in the mPFC and vHPC. Microinjecting Tat-SERT-15C, but not fluoxetine, into the DRN reversed the CMS-induced decrease in intercellular 5-HT in the mPFC and vHPC 2 hours after treatment (Fig. 3F).

Next, we microinjected AAV9-DIO-hM4Di-GFP virus into the DRN of SERT-Cre mice and implanted a cannula in the mPFC or vHPC. Four weeks later, we treated the mice with Tat-SERT-15C intraperitoneally and infused CNO into the mPFC or vHPC through a cannula 2 hours before the behavioral tests (Fig. 3G). GFP-labeled projection fibers observation showed DRN-mPFC (5-HT<sup>DRN-mPFC</sup>) and DRN-vHPC (5-HT<sup>DRN-vHPC</sup>) serotonergic circuits (Fig. 3H). Silencing the 5-HT<sup>DRN-mPFC</sup> circuit by CNO abolished the antidepressant-like effect of Tat-SERT-15C, but silencing the 5-HT<sup>DRN-vHPC</sup> circuit did not (Fig. 3I). Microinjection of either CNO or Tat-SERT-15C into the mPFC of WT mice did not induce a depression-associated behavior change at 2 hours (fig. S5C). Additionally, neither ketamine nor fluoxetine treatment altered SERT-nNOS coupling in the



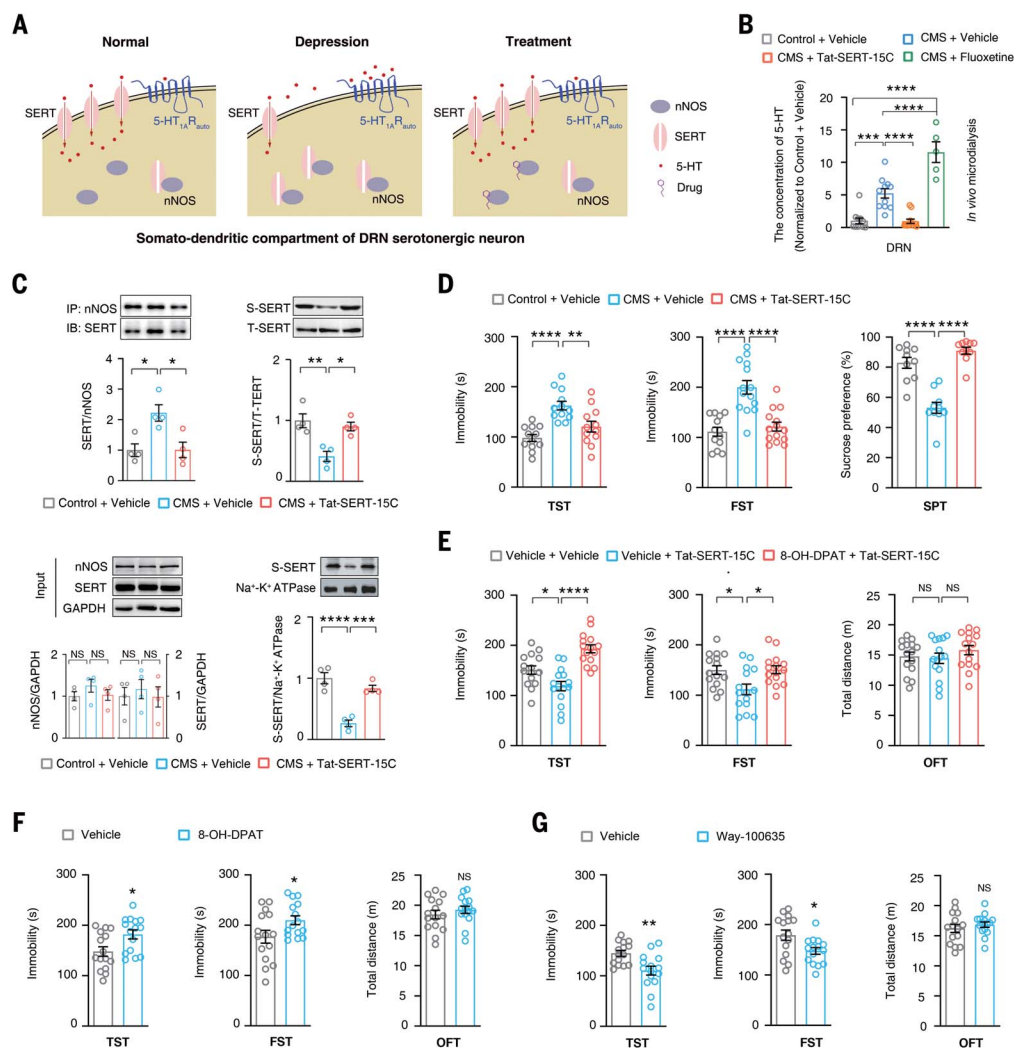


**Fig. 2. Dissociating SERT from nNOS in the DRN reverses CMS-induced depressive behaviors.** (A) Sketch describing our hypothesis: chronic stressors reduce the cell surface translocation of SERT by promoting a SERT-nNOS association, thereby increasing intercellular 5-HT concentration, facilitating the activation of DRN somatodendritic 5-HT<sub>1A</sub>R<sub>auto</sub>s, and causing depression. Dissociating SERT from nNOS may reverse this pathological process. (B) Microinjection of Tat-SERT-15C (1.6  $\mu$ g) but not fluoxetine (2  $\mu$ g) into the DRN reversed CMS-induced elevated intercellular 5-HT in the DRN at 2 hours as measured by in vivo microdialysis ( $n = 5$  to 13 mice; data were analyzed with one-way ANOVA). (C) Microinjection of Tat-SERT-15C (1.6  $\mu$ g) into the DRN reversed 28d-CMS-induced SERT-nNOS overcoupling and reduced translocation on the cellular membrane in the DRN at 2 hours. The expression of nNOS and SERT in the DRN were not affected

DRN (fig. S6, A and B). RNA-sequencing data showed that microinjection of Tat-SERT-15C into the DRN and intraperitoneal injection of ketamine or fluoxetine affected different profiles of gene expression in the mPFC (fig. S6, C and D), suggesting that they have different underlying mechanisms.

#### Small-molecule fast-onset antidepressant drug designed by dissociating SERT from nNOS

To find small molecules that selectively dissociate SERT from nNOS, we analyzed the chemical mechanism of binding the C-tail of SERT

to the PDZ of nNOS in the DRN and, based on this, designed a common chemical structure (Fig. 4A). Using cultured 293T cells transfected with plasmids encoding nNOS and SERT, we detected the effects of a series of compounds on the SERT-nNOS interaction (fig. S7). The quantitative structure-activity relationship indicated that the chemical structure of Ac-Ala-Val-OH, tightly bound into the groove between the  $\alpha$ B helix and  $\beta$ B folding of the nNOS PDZ domain and the L configuration of Val, was crucial for blocking SERT-nNOS. Steric hindrance caused by large groups on the ester may be

( $n = 4$  mice; data were analyzed by one-way ANOVA). (D) Microinjection of Tat-SERT-15C (1.6  $\mu$ g) into the DRN rescued depressive behaviors of CMS-exposed mice in TST, FST, and sucrose preference test at 2 hours.  $n = 10$  to 14 mice; data were analyzed by one-way ANOVA). (E) Microinjecting 8-OH-DPAT (1  $\mu$ g) into the DRN through a previously implanted cannula, followed by Tat-SERT-15C treatment (5 mg/kg, intraperitoneally) at 5 min. TST, FST, and OFT were performed 2 hours later ( $n = 15$  mice; data were analyzed by one-way ANOVA). (F) TST, FST, and OFT 2 hours after microinjecting 8-OH-DPAT (1  $\mu$ g) or vehicle into the DRN ( $n = 15$  mice; data were analyzed by Student's  $t$  test). (G) TST, FST, and OFT 2 hours after microinjecting Way-100635 (3  $\mu$ g) or vehicle into the DRN ( $n = 15$  mice; data were analyzed using Student's  $t$  test). \* $P < 0.05$ ; \*\* $P < 0.01$ ; \*\*\* $P < 0.001$ ; \*\*\*\* $P < 0.0001$ ; NS, not significant. Error bars indicate SEM.

disadvantageous for binding into nNOS PDZ domain, and the chirality of Ala did not affect the binding activity (Fig. 4, B and C, and fig. S7A). Of these compounds, ZZL-7 had advantageous structural characteristics: The acetylated amino of Ala of ZZL-7 formed an H-bond with Phe<sup>24</sup> of nNOS with a 2.11-Å bond distance; the carbonyl of Val of ZZL-7 made two H-bonds with the guanidino of Arg<sup>79</sup> of nNOS with 1.96-Å, 2.18-Å, respectively; and there was a hydrophobic interaction between the methyl of acetyl and the benzene ring of Phe<sup>24</sup> of nNOS (Fig. 4, A to C, and fig. S7B).

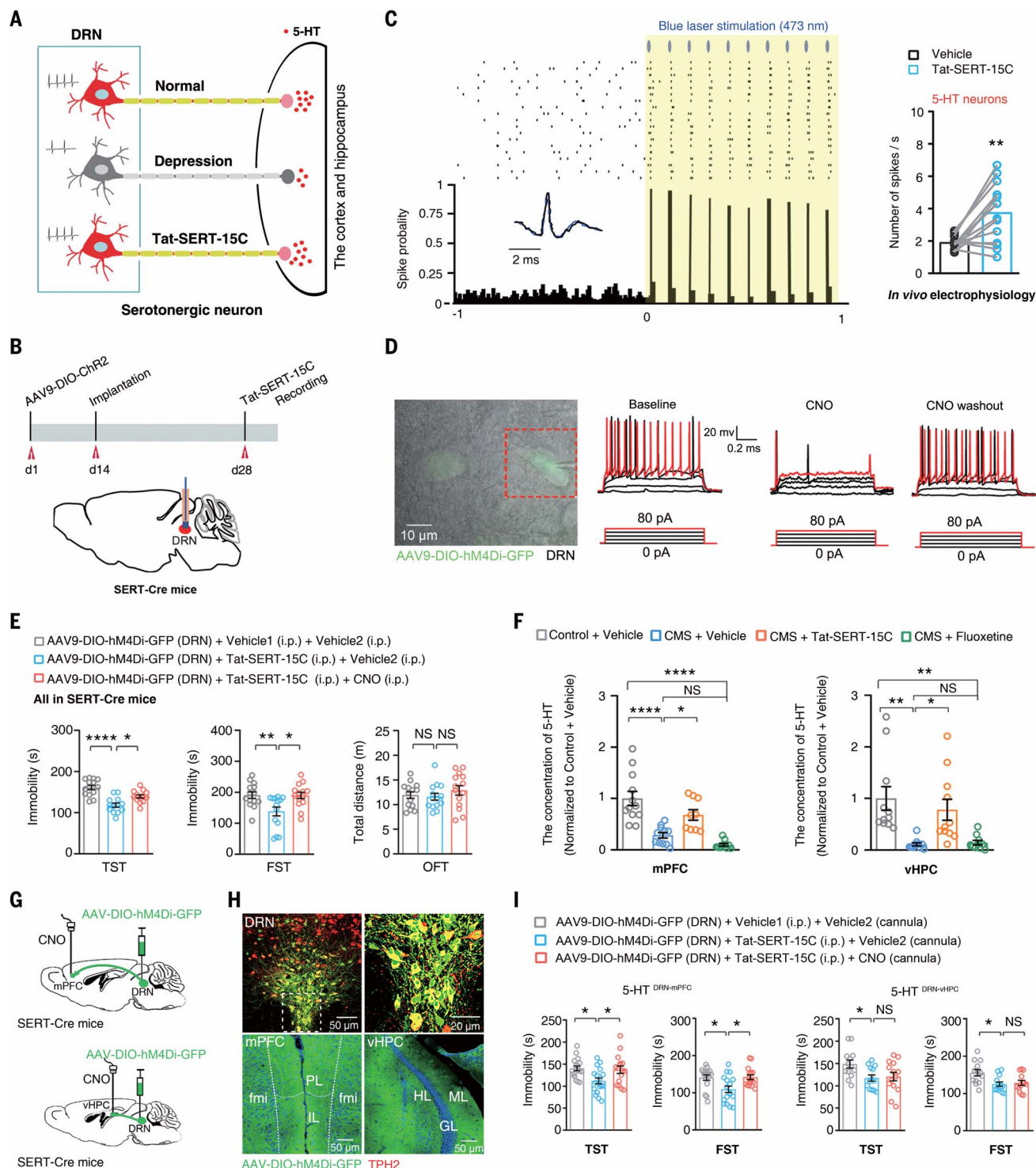


**Fig. 3. Circuit mechanism mediates the antidepressant effect produced by dissociating SERT-nNOS.** (A) Diagrammatic sketch of our hypothesis.

(B) A volume of 0.5  $\mu$ l of AAV9-DIO-ChR2 was microinjected into the DRN of 2-month-old SERT-Cre mice, followed by implantation of a photogenetic lens and an in vivo electrophysiological recording electrode 14 d later. Two weeks later, Tat-SERT-15C (5 mg/kg, intraperitoneally) was administered 2 hours before recording. (C) The recording of neural firing of serotonergic neurons was validated by blue laser (473 nm) stimulation ( $n = 14$  neurons from  $n = 3$  mice; data were analyzed by paired Student's  $t$  test). (D) A volume of 0.5  $\mu$ l of AAV9-DIO-hM4Di-GFP was microinjected into the DRN of 2-month-old SERT-Cre

mice. One month later, mice were treated with Tat-SERT-15C (5 mg/kg, intraperitoneally) or vehicle1 (saline) with or without CNO (5 mg/kg, intraperitoneally) or vehicle2. Brain slices were prepared 2 hours after treatment for in vitro electrophysiology recording. Data are representative of 10 individual neurons. (E) Mice behavior in the TST, FST, and OFT 2 h after treatments ( $n = 13$  to 14 mice; data were analyzed by one-way ANOVA). (F) Microinjection of Tat-SERT-15C (1.6  $\mu$ g) but not fluoxetine (2  $\mu$ g) reversed the CMS-induced decrease of intercellular 5-HT in the mPFC and vHPC at 2 hours, as measured by in vivo microdialysis ( $n = 9$  to 12 mice; data were analyzed by one-way ANOVA). (G) Design of the selective deactivation of the 5-HT<sup>DRN-mPFC</sup> or 5-HT<sup>DRN-vHPC</sup>

circuit. **(H)** Infection status 1 min after injection of AAV9-DIO-hM4Di-GFP into the DRN of SERT-Cre mice. Note the projected GFP<sup>+</sup> serotonergic fibers in the mPFC and vHPC ( $n = 5$  mice). **(I)** Behavior in the TST and FST 2 hours after CNO (2  $\mu$ g) infusion into the mPFC or vHPC through a previously implanted cannula in

SERT-Cre mice ( $n = 13$  to 18 mice; data were analyzed by one-way ANOVA). \* $P < 0.05$ ; \*\* $P < 0.01$ ; \*\*\* $P < 0.001$ ; \*\*\*\* $P < 0.0001$ ; NS, not significant. Error bars indicate SEM. PL/IL, prelimbic/infralimbic area of the mPFC; fmi, forceps minor of the corpus callosum; HL, hilus; ML, molecular layer; GL, granule layer.

Incubation of the cultured 293T cells transfected with nNOS and SERT with ZYL-7 for 2 h significantly decreased the SERT-nNOS complex level (Fig. 4D). In vivo electrophysiology in SERT-Cre mice showed that ZYL-7 caused significantly increased firing frequency of serotonergic neurons 2 hours after treatment (Fig. 4E). In WT mice, ZYL-7 reduced immobility time as shown by TST and FST 2 hours after systematic administration, suggesting a fast antidepressant-like effect. In *nNos*<sup>-/-</sup> mice, however, the treatment did not affect immobility time in the TST and FST (fig. S7C). Treatment with ZYL-7 caused a significantly decreased SERT-nNOS complex level and an increased cell surface SERT level in the DRN in WT but not in *nNos*<sup>-/-</sup> mice (fig. S7D). Intragastric administration of ZYL-7 produced antidepressant-like behaviors dose dependently 2 hours after treatment (Fig. 4F). To investigate whether ZYL-7 could elicit a fast-onset antidepressant effect in depressed mice, we injected ZYL-7 intravenously to 28d-CMS-experienced mice. As expected, ZYL-7 reversed the CMS-induced increase in the SERT-nNOS complex in the DRN (Fig. 4G) and reversed CMS-induced depressions behaviors 2 hours after treatment (Fig. 4H). The fast-onset antidepressant effect persisted at least for 24 hours (fig. S8A). At 30 min after administration of ZYL-7, ZYL-7 was detected in the DRN tissue, indicating that it crossed the blood-brain barrier readily (fig. S8B). We incubated 293T cells with ZYL-7 and washed out the culture medium 30, 60, 90, and 120 min later. Liquid chromatography-mass spectrometry analysis of compound composition in the cytoplasm demonstrated that ZYL-7 also penetrated the cellular membrane (fig. S8, C and D).

ZYL-7 had no effect on general activity or locomotor activity, memory, or cognition (fig. S9, A to F) and did not induce aggressive behavior, addiction, or abnormal brain waves (fig. S9, G to I). Our results suggest that ZYL-7 should be developed as a new, fast-onset antidepressant candidate. All of the uncropped Western blots are shown in fig. S10.

## Discussion

Significantly increased 5-HT concentration, somatodendritic 5-HT<sub>1A</sub>R<sub>auto</sub> level, and 5-HT<sub>1A</sub>R<sub>auto</sub> binding rate in the DRN are related to MDD and suicide attempts (19). Suppression of 5-HT<sub>1A</sub>R<sub>auto</sub>s evokes strong and rapid antidepressant-like effects (21). Rapid DRN 5-HT<sub>1A</sub>R<sub>auto</sub> desensitization or knockdown can accelerate the onset of the therapeutic effects of antidepressants (32, 33). Therefore,

selectively blocking DRN 5-HT<sub>1A</sub>R<sub>auto</sub>s could be a strategy for discovering fast-onset antidepressants. However, how to selectively manipulate DRN 5-HT<sub>1A</sub>R<sub>auto</sub>s without affecting postsynaptic 5-HT<sub>1A</sub>R<sub>heter</sub>s remains unresolved. If intercellular 5-HT in the DRN could be selectively reduced, then DRN 5-HT<sub>1A</sub>R<sub>auto</sub> function could be selectively suppressed. We discovered that dissociating SERT from nNOS specifically reduces intercellular 5-HT concentration in the DRN by facilitating the cell surface translocation of SERT, enhances DRN serotonergic neurons activity, and substantially promotes 5-HT release into the mPFC, thereby producing a fast-onset antidepressant effect. Further, the small molecule SNIB ZYL-7 that we designed had a fast-onset antidepressant effect in our mouse depression model.

Current antidepressants such as fluoxetine, which work as selective serotonin reuptake inhibitors (SSRIs), have no selectivity in inhibiting somatodendritic SERT in the DRN or presynaptic SERT in nerve terminals. They also have no preference in enhancing the functions of DRN 5-HT<sub>1A</sub>R<sub>auto</sub>s and postsynaptic 5-HT<sub>1A</sub>R<sub>heter</sub>s in the cortex and HPC (34). Because of the enhancement of DRN 5-HT<sub>1A</sub>R<sub>auto</sub> function caused by inhibiting somatodendritic SERT, SSRIs suppress neural firing and 5-HT release of serotonergic neurons (16, 35). The effects of SSRIs depend on the desensitization of DRN 5-HT<sub>1A</sub>R<sub>auto</sub>s (16, 21, 36). The desensitization of 5-HT<sub>1A</sub>R<sub>auto</sub>s explains the drawbacks of SSRIs, including third delayed onset, unstable effectiveness, individual differences, and even aggravating symptoms (19, 33, 34). By contrast, SNIBs work by reducing intercellular 5-HT and thereby deactivating DRN 5-HT<sub>1A</sub>R<sub>auto</sub>s without the requirement for desensitization, thus potentially avoiding the deficits of SSRIs.

The concentration of intercellular 5-HT in the DRN is critically regulated by SERT on the cell surface. SERT is a natural ligand of the nNOS PDZ domain and can bind to the pocket constituted by the  $\alpha$ B helix and  $\beta$ B fold of this domain through its C-terminal peptides (22). The binding site on the nNOS PDZ domain is a shallow and long groove containing the binding pocket of the conserved sequence GLGF (Gly<sup>21</sup>, Leu<sup>22</sup>, Gly<sup>23</sup>, Phe<sup>24</sup>) (37). The C-terminal residue of SERT also binds transport molecules Sec23A and Sec24C, two subunits of coat complex II, which is critical for the trafficking of SERT to the plasma membrane, and nNOS may compete with Sec23-Sec24 for binding to the SERT C terminus (22). Therefore, the fast-onset

antidepressant effect of SNIBs may be explained by the fact that the dissociation of SERT-nNOS facilitates Sec23-Sec24-mediated trafficking of SERT to the cell surface, thereby reducing intercellular 5-HT and in turn down-regulating 5-HT<sub>1A</sub>R<sub>auto</sub> activity.

The limitations of ketamine, including neurotoxicity, cognitive dysfunction, abnormal mental status, and psychotomimetic effects, have been reported (38). Although ketamine is a noncompetitive antagonist of the *N*-methyl-D-aspartate receptor, it also binds on many other receptors, with potentially extensive pharmacological effects and side effects (39). Our data showed that ketamine had no effect on SERT-nNOS association, and the gene expression profile was differently regulated by ketamine and SNIB. Therefore, SNIBs may produce a fast-onset antidepressant effect without the drawbacks of ketamine.

The mPFC is closely related to rapid antidepressant responses (40–43). The activity of mPFC is significantly elevated during periods of struggling in depression-related behavior tests including TST and FST (44). Ketamine acutely increases the activity of mPFC pyramidal neurons (45). Neuronal vascular endothelial growth factor (VEGF) and mammalian target of rapamycin (mTOR) signaling in the mPFC are the mediators of ketamine's rapid antidepressant effects (46, 47). Intra-mPFC infusion of 8-OH-DPAT induces rapid and long-lasting antidepressant-like effects (48). We found that the activity of the 5-HT<sup>DRN-mPFC</sup> circuit contributes to the fast-onset antidepressant effect of SNIBs. Consistent with previous reports (49, 50), our data suggest that the 5-HT<sup>DRN-vHPC</sup> circuit may be implicated in the chronic antidepressant effect of SNIBs.

The level of SERT as part of the SERT-nNOS complex and the fraction of total SERT protein in the DRN are much higher than in other depression-associated brain regions. The selective existence and formation of SERT-nNOS are possibly due to the predominant and intensive expression of SERT in the DRN and the selective postsynaptic location of nNOS in the synaptic terminal regions of serotonergic neurons (51, 52). In these regions, presynaptic membrane SERT is the target of SSRIs, and nNOS is found (51–53). Although a few SERT-nNOS complexes are detected in the fibers of serotonergic neurons, such as those in the mPFC, the interaction is predominantly located in the cell body (54, 55), and our results suggest that the SERT-nNOS complex in the mPFC is not implicated in depression. Moreover, there was no evidence for the existence



**Fig. 4. Development of a small-molecule drug eliciting rapid-onset anti-depressant effect.** (A) Top:

general structure with potential bioactivity to uncouple nNOS and SERT. Bottom: structure of ZZL-7.

(B and C) ZZL-7 (Ac-Ala-Val-OCH<sub>3</sub>) was tightly bound into the groove between the  $\alpha$ B helix and  $\beta$ B folding of the nNOS PDZ domain. In the ZZL-7-nNOS PDZ domain complex, there was a hydrogen bonding interaction between the ZZL-7 and GLGF loop (Gly<sup>21</sup>-Leu<sup>22</sup>-Gly<sup>23</sup>-Phe<sup>24</sup>) of the nNOS PDZ domain. The acetylated amino of Ala (ZZL-7) formed a H-bond with Phe<sup>24</sup>; the H-bond distance was 2.11 Å. The  $\gamma$ -carbonyl of Val made two H-bonds with the guanidino of Arg<sup>79</sup> and H-bond distances were 1.96 Å, 2.41 Å. (D) Co-IP showing SERT-nNOS complex levels in 293T cells incubated with 1.0  $\mu$ M ZZL-7 for 2 hours ( $n = 5$  mice; data were analyzed by Student's  $t$  test).

(E) Enhanced firing frequency of serotonergic neurons 2 hours after ZZL-7 administration (10 mg/kg, intraperitoneally) in SERT-Cre mice detected by *in vivo* electrophysiology ( $n = 15$  neurons measured from  $n = 3$  individual mice; data were analyzed by paired Student's  $t$  test). (F) Mouse behavior in the TST and FST 2 hours after intragastric administration of ZZL-7 (10, 20, and 40 mg/kg).

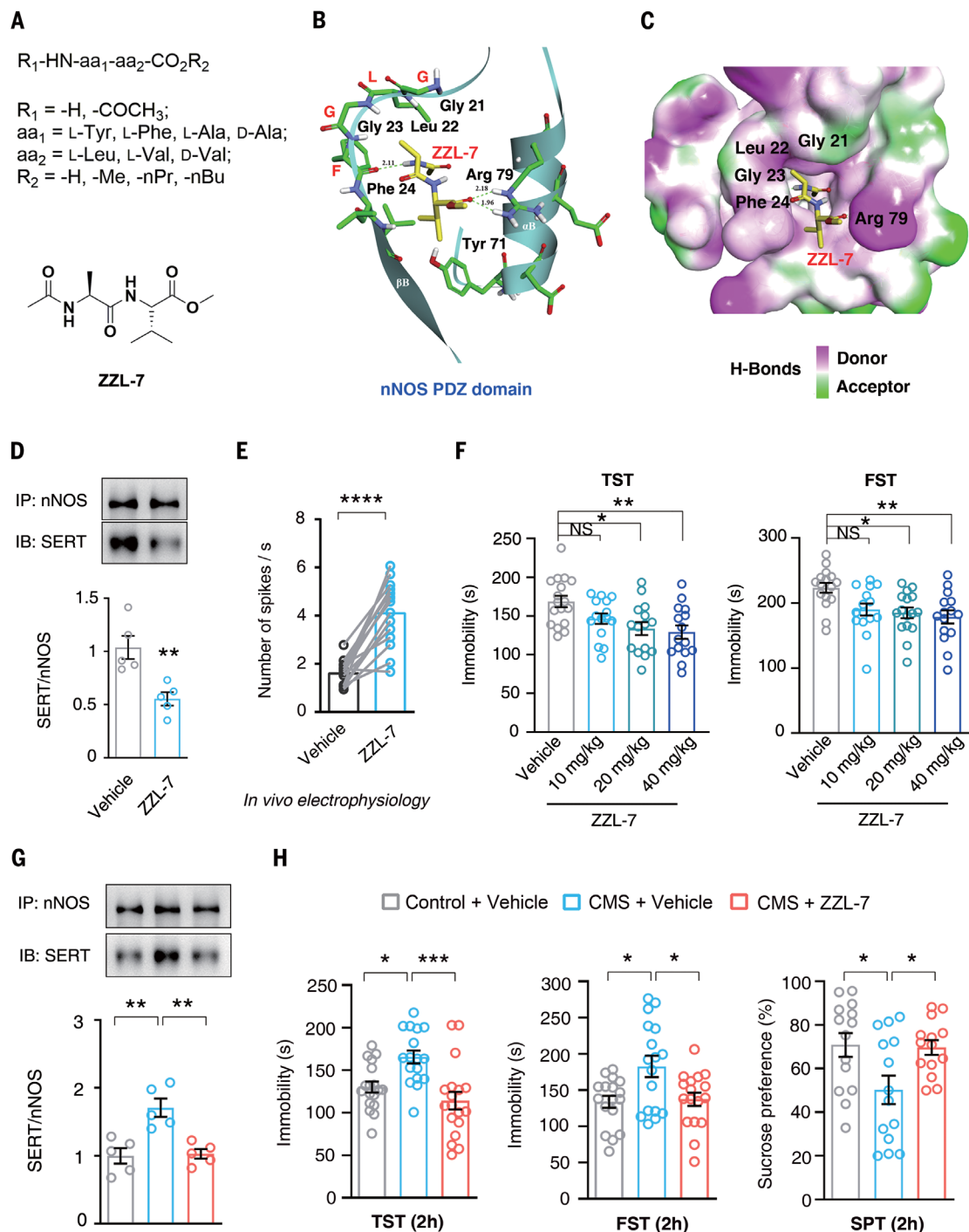
(G) SERT-nNOS complex level in the DRN of 28d-CMS-exposed or control mice 2 hours after intraperitoneal administration of ZZL-7 (10 mg/kg) ( $n = 5$  mice; data were analyzed by one-way ANOVA). (H) TST, FST, and sucrose preference test in 28d-CMS-exposed or control mice 2 hours after intraperitoneal administration of ZZL-7 (10 mg/kg) ( $n = 14$  to 18 mice; data were analyzed by one-way ANOVA). \* $P < 0.05$ ; \*\* $P < 0.01$ ; \*\*\* $P < 0.001$ ; NS, not significant. Error bars indicate SEM.

of SERT-nNOS complexes outside of the brain, such as in the gut, platelets, and the immune system. Therefore, SNIBs may selectively target the DRN, thus avoiding undesirable pharmacological effects.

Furthermore, although a large number of protein-protein interaction inhibitors have been

reported, compounds that promote protein-protein interactions are rare. We found here that Sakura can promote the SERT-nNOS association. We deduce that Sakura may act as a linker of the nNOS PDZ domain and SERT and thereby facilitate the SERT-nNOS interaction, because it not only forms several H-bonds

with Lys<sup>27</sup>, Tyr<sup>71</sup>, and Arg<sup>79</sup> on the nNOS PDZ domain, but also binds to SERT through H-bond and hydrophobic interactions. For example, there is a hydrophobic interaction between the side chain of Met<sup>627</sup> in SERT and the cyclohexylethyl of Sakura, the carbonyl of Ala<sup>629</sup> in SERT forms an H-bond with Lys<sup>27</sup> of



nNOS PDZ, the side chain of Val<sup>630</sup> in SERT has a hydrophobic interaction with Leu<sup>25</sup> of the nNOS PDZ, and the carboxyl of Val<sup>630</sup> in SERT can form an H-bond with indole of Trp on Sakura.

In sum, we show here that dissociating SERT-nNOS can rapidly reverse the depressive behaviors caused by CMS in mice, opening a new avenue for developing therapeutics for mood disorders, which should now be tested in humans.

## Methods summary

### Mice

Male C57BL/6J (8 to 12 weeks old, 20 to 25 g, stock no. 000664), *Tph2*-CreER (stock no. 016584), *nNos*<sup>-/-</sup> (stock no. 002986), and SERT-Cre (stock no. 014554) mice were purchased from the Jackson Laboratory (Bar Harbor, ME, USA) and maintained at the Model Animal Research Center of Nanjing Medical University (Nanjing, China). The *nNos*<sup>flox/flox</sup> mice (C57BL/6J background), exons 4 to 7 with loxP recombination sites, were generated by CRISPR genome editing technology (CRISPR-Cas9 system) and maintained at the Model Animal Research Center of Nanjing University (Nanjing, China). Conditional knockout of *nNos* in serotonergic neurons (*nNos* CKO) was established by crossing *Tph2*-CreER mice with *nNos*<sup>flox/flox</sup> mice to generate *Tph2*-CreER; *nNos*<sup>flox/flox</sup> mice, treated with tamoxifen (150 mg/kg subcutaneously for 3 days) when mice were 2 months old. Behavior tests and immunofluorescence were performed 1 month later. Every effort was made to minimize pain and suffering, and we reduced the number of animals used in the experiments. Mice were housed five per cage under standard laboratory conditions (22 ± 1°C, 60% humidity, 12 h light-dark cycle with lights on at 7:00 a.m., food and water ad libitum) for 1 week before starting experiments. All procedures concerning animal care and treatment were performed in accordance with the protocols approved by the ethical committee of Nanjing Medical University (protocol no. IACUC-1704010-1).

### Drugs and polypeptides

ZZL molecules and Sakura were designed and synthesized by the Ting-You Li laboratory at the Department of Pharmacochimistry, Nanjing Medical University (Nanjing, China). CNO, Way-100635, and 8-OH-DPAT were purchased from Sigma-Aldrich (St. Louis, MO, USA) and intraperitoneally injected (10 mg/kg) or locally microinjected into the mPFC or vHPC to activate hM4Di DREADD receptors. Dimethyl sulfoxide (0.5%) in saline was used as a vehicle (referred to as “vehicle2” in Fig. 3) (56). To selectively knock out the *nNos* gene in serotonergic neurons in *Tph2*-CreER; *nNos*<sup>flox/flox</sup> mice, tamoxifen (150 mg/kg, intraperitoneally, dissolved in a 1:10 mixture of ethanol and

sunflower oil, Sigma-Aldrich) was administered daily for 3 days when the mice were 2 months old (56). Fluoxetine and (2R,6R)-hydroxynorketamine hydrochloride were purchased from Sigma-Aldrich and Jiangsu Pharmaceutical Co., Ltd. (Jiangsu, China), dissolved in saline, and administered as approved by the Food and Drug Administration of Jiangsu Province (2018). A cannula was implanted into the DRN, mPFC, or vHPC and used for microinjection of drugs or peptides 3 d later. During microinjection, mice were anesthetized temporarily for 5 min by isoflurane (induction 3%, 0.8 liters/min O<sub>2</sub>; maintenance 1 to 1.5%, 0.5 liters/min O<sub>2</sub>).

### Microdialysis

The microdialysis methods used in the construction of guide cannula and probes have been previously described (57). Under isoflurane anesthesia, all animals underwent a stereotactic surgical procedure for placement of a polysulfone recording chamber (Crist Instruments, Damascus, MD), in the DRN, mPFC, or vHPC, which directs the insertion of the microdialysis probes. Microdialysis probes were placed in sites that had not been previously sampled the day before the experiment. After lowering the probe, a protective cap was used to cover the chamber overnight. The following day, the cap was removed, and inlet and outlet lines were attached to the probe for microdialysis. Probes were held in place snugly and were prevented from rotating by using a tab. The solution used to perfuse the probe at 1.0 µl/min contained the following (in mM): KCl 2.4, NaCl 137, CaCl<sub>2</sub> 1.2, MgCl<sub>2</sub> 1.2, and NaH<sub>2</sub>PO<sub>4</sub> 0.9, pH 7.4, ascorbate 0.2. The levels of serotonin, noradrenalin, and dopamine in the perfusates were then determined using liquid chromatography-mass spectrometry. Using these procedures, dialysate transmitters were sampled every 10 min from the regions of interest at baseline and after treatments.

### Coimmunoprecipitation and pull-down analysis

Procedures for coimmunoprecipitation and pull-down analysis were previously described (24). The DRN or cultured 293T cells were lysed and centrifuged. The supernatant was preincubated with protein G-Sepharose beads (Sigma-Aldrich) and then centrifuged to obtain the target supernatant. Antibody-conjugated protein G-Sepharose beads were incubated with the target supernatant, centrifuged, washed, and heated to elute bound proteins, and proteins were analyzed by immunoblotting. For more details, see the supplementary materials.

### Stereotaxic injection

The surgical procedure was performed as described previously (58), with additional changes to the injection coordinates. Under isoflurane anesthesia, stereotactic surgery was per-

formed to deliver virus or solution into the DRN and to implant cannulas into the DRN, mPFC, or vHPC using the following coordinates: DRN, AP = 0 mm, ML = 0 mm, DV = 3.0 mm, from lambda; mPFC, AP = +1.8 mm, ML = ± 0.3 mm, DV = 2.1 mm; vHPC, AP = -2.9 mm, ML = ± 2.8 mm, DV = -3.6 mm, from bregma. A volume of 200 nl of drugs or 500 nl of viruses was microinjected into brain regions. A motorized stereotaxic injector (Stoelting, model no. 53311) was used to infuse virus at a rate of 0.2 µl/min.

### Design and synthesis of ZZL-7

H-Ala-Val-OH was the C-terminal dipeptide of SERT, which was potential as a small-molecule blocker of SERT/nNOS interaction. In view of the poor stability of enzymatic hydrolysis and the blood-brain barrier permeability of H-Ala-Val-OH, acetylated alanine and esterified Val were used to form ZZL-7 (Ac-Ala-Val-OMe). ZZL-7 has the advantages of small molecular weight and being easy to synthesize. ZZL-7 was obtained by following the next synthetic steps. To a solution of Boc-Ala-OH (4 g, 21.1 mmol) and H-Val-OMe-HCl (3.9 g, 23.3 mmol) in anhydrous DMF (50 ml), DIPEA (9.3 ml, 53.3 mmol) and PyBOP (12 g, 23.3 mmol) were added at 0°C. The mixture was stirred overnight at room temperature. The solvent was removed in vacuo. The residue was dissolved in EA (100 ml), washed with 10% citric acid (3 × 40 ml), 5% NaHCO<sub>3</sub> (3 × 40 ml), and brine (2 × 40 ml), dried over Na<sub>2</sub>SO<sub>4</sub>, and concentrated in vacuo. The crude product was purified by silica gel chromatography (PE: EA=2:1) to give Boc-Ala-Val-OMe (6.07 g, 95%) as a white solid. <sup>1</sup>H nuclear magnetic resonance (<sup>1</sup>H NMR) imaging (400 MHz, CDCl<sub>3</sub>): δ 6.96 (d, *J* = 8.0 Hz, 1H), 5.40 (d, *J* = 6.7 Hz, 1H), 4.54 (q, *J* = 8.9 Hz, 1H), 4.34–4.16 (m, 1H), 3.74 (s, 3H), 2.14–2.22 (m, 1H), 1.45 (s, 9H), 1.36 (d, *J* = 7.0 Hz, 3H), and 0.92 (dd, *J* = 10.9, 6.9 Hz, 6H). A solution of Boc-Ala-Val-OMe (6 g, 19.8 mmol) in 80.6 ml (386.9 mmol) of hydrochloride dioxane (4.8 mol/L) was stirred at room temperature for 2 hours. After completion of the reaction, the solution was concentrated in vacuo to obtain the crude H-Ala-Val-OMe-HCl.

DIPEA (6.9 ml, 39.7 mmol) was added to a solution of H-Ala-Val-OMe-HCl and Ac<sub>2</sub>O (2.8 ml, 29.8 mmol) in THF at 0°C. The mixture was stirred for 10 min and then warmed to room temperature to stir for 2 hours. The solvent was concentrated in vacuo. The residue was dissolved in EA and washed with 10% citric acid, 5% NaHCO<sub>3</sub>, and brine, dried over Na<sub>2</sub>SO<sub>4</sub>, and concentrated in vacuo. The crude product was purified by silica gel chromatography (CH<sub>2</sub>Cl<sub>2</sub>: MeOH = 30:1) to give ZZL-7 (Ac-Ala-Val-OMe, 3.6 g, 74%) as a white solid. <sup>1</sup>H NMR (400 MHz, CDCl<sub>3</sub>): δ 6.77 (d, *J* = 8.4 Hz, 1H), 6.30 (d, *J* = 6.9 Hz, 1H), 4.59 (p, *J* =



7.0 Hz, 1H), 4.50 (dd,  $J = 8.7, 5.0$  Hz, 1H), 3.75 (s, 3H), 2.24–2.13 (m, 1H), 2.00 (s, 3H), 1.38 (d,  $J = 6.9$  Hz, 3H), 0.92 (dd,  $J = 9.4, 6.9$  Hz, 6H).  $^{13}\text{C}$  NMR (101 MHz,  $\text{CDCl}_3$ )  $\delta$  172.43, 172.19, 170.03, 57.39, 52.24, 48.90, 31.11, 23.17, 19.01, 18.32, 17.74. MS (ESI) calculated for  $\text{C}_{11}\text{H}_{19}\text{N}_2\text{O}_4$   $[\text{M}-\text{H}]^-$  was 243.13; found:  $m/z$  243.2.

## Statistics

All data were analyzed using Prism 8 software (GraphPad Software, Cary, NC, USA). After a homogeneity test of variance, when equal variances were assumed, unpaired or paired Student's  $t$  test was used to estimate the differences between two groups, one-way ANOVA was used for comparison among three or four groups, and two-way ANOVA with Bonferroni's multiple-comparisons corrections was used to compare the effect of two factors with respect to a numeric outcome. The results were considered significant at  $P < 0.05$ . All experimental results are shown as mean  $\pm$  SEM. Sample sizes were based on previous studies in this field. Outliers were excluded according to the analysis of identify outliers using Prism software. Animals were randomly assigned to experimental groups. The investigator was blinded to the group allocation during the experiment and/or when assessing the outcome. Statistical parameters, including  $n$ ,  $t$ , and  $F$  values and  $P$  values, and the analytical method used for each experiment, are listed in the supplementary materials.

## Additional methods

Detailed methodology, including electrophysiological recordings, viral production, behavioral testing, CMS model, Western blot analysis, and drug concentration determination are described in the supplementary materials.

## REFERENCES AND NOTES

- H. Herrman et al., *Lancet* **399**, 957–1022 (2022).
- D. L. Murphy, K. P. Lesch, *Nat. Rev. Neurosci.* **9**, 85–96 (2008).
- D. Chancellor, *Nat. Rev. Drug Discov.* **10**, 809–810 (2011).
- J. Licinio, M. L. Wong, *Nat. Rev. Drug Discov.* **4**, 165–171 (2005).
- I. Maany, *JAMA* **292**, 2833, author reply 2833 (2004).

- E. T. Kavalali, L. M. Monteggia, *Curr. Opin. Pharmacol.* **20**, 35–39 (2015).
- K. M. Bozymski et al., *Ann. Pharmacother.* **54**, 567–576 (2020).
- R. B. Price, M. K. Nock, D. S. Charney, S. J. Mathew, *Biol. Psychiatry* **66**, 522–526 (2009).
- C. G. Abdallah, G. Sanacora, R. S. Duman, J. H. Krystal, *Annu. Rev. Med.* **66**, 509–523 (2015).
- E. J. Daly et al., *JAMA Psychiatry* **75**, 139–148 (2018).
- A. C. Hayley, C. Stough, J. C. Verster, A. J. van de Loo, L. A. Downey, *Curr. Drug Abuse Rev.* **8**, 1–2 (2015).
- O. Lipsitz et al., *Am. J. Geriatr. Psychiatry* **29**, 899–913 (2021).
- K. A. Trujillo, S. D. Iñiguez, *Behav. Brain Res.* **394**, 112841 (2020).
- P. R. Albert, B. Le François, A. M. Millar, *Mol. Brain* **4**, 21 (2011).
- B. W. Okaty, K. G. Commons, S. M. Dymecki, *Nat. Rev. Neurosci.* **20**, 397–424 (2019).
- J. W. Richardson-Jones et al., *Neuron* **65**, 40–52 (2010).
- H. Gozlan, S. El Mestikawy, L. Pichat, J. Glowinski, M. Hamon, *Nature* **305**, 140–142 (1983).
- J. D. Coplan, S. Gopinath, C. G. Abdallah, B. R. Berry, *Front. Behav. Neurosci.* **8**, 189 (2014).
- C. A. Stockmeier et al., *J. Neurosci.* **18**, 7394–7401 (1998).
- M. L. Wong, J. Licinio, *Nat. Rev. Drug Discov.* **3**, 136–151 (2004).
- A. Bortolozzi et al., *Mol. Psychiatry* **17**, 612–623 (2012).
- B. Channion et al., *Proc. Natl. Acad. Sci. U.S.A.* **104**, 8119–8124 (2007).
- L. J. Zhu et al., *Nat. Med.* **20**, 1050–1054 (2014).
- L. Zhou et al., *Nat. Med.* **16**, 1439–1443 (2010).
- C. Qin et al., *Mol. Psychiatry* **26**, 6506–6519 (2021).
- Y. Qin et al., *ACS Chem. Neurosci.* **12**, 244–255 (2021).
- K. A. Michelsen, J. Prickaerts, H. W. M. Steinbusch, *Prog. Brain Res.* **172**, 233–264 (2008).
- P. E. Lutz, *J. Neurophysiol.* **109**, 2245–2249 (2013).
- Y. Sato, I. Sagami, T. Shimizu, *J. Inorg. Biochem.* **87**, 261–266 (2001).
- P. Blier, G. Piñeyro, M. el Mansari, R. Bergeron, C. de Montigny, *Ann. N. Y. Acad. Sci.* **861** (1 ADVANCES IN S), 204–216 (1998).
- G. Piñeyro, P. Blier, *Pharmacol. Rev.* **51**, 533–591 (1999).
- A. Ferrés-Coy et al., *Psychopharmacology* **225**, 61–74 (2013).
- J. M. Watson, L. A. Dawson, *CNS Drug Rev.* **13**, 206–223 (2007).
- N. A. Gray et al., *Biol. Psychiatry* **74**, 26–31 (2013).
- J. A. Stamford, C. Davidson, D. P. McLaughlin, S. E. Hopwood, *Trends Neurosci.* **23**, 459–465 (2000).
- E. Quentin, A. Belmer, L. Maroteaux, *Front. Neurosci.* **12**, 982 (2018).
- H. Tochio, Q. Zhang, P. Mandal, M. Li, M. Zhang, *Nat. Struct. Biol.* **6**, 417–421 (1999).
- B. Short, J. Fong, V. Galvez, W. Shelker, C. K. Loo, *Lancet Psychiatry* **5**, 65–78 (2018).
- P. Zanos et al., *Pharmacol. Rev.* **70**, 621–660 (2018).
- M. V. Fogaça et al., *Mol. Psychiatry* **26**, 3277–3291 (2021).
- E. S. Wohleb et al., *J. Clin. Invest.* **126**, 2482–2494 (2016).
- T. Kato et al., *J. Clin. Invest.* **129**, 2542–2554 (2019).
- B. D. Hare et al., *Nat. Commun.* **10**, 223 (2019).
- R. N. Moda-Sava et al., *Science* **364**, eaat8078 (2019).
- B. D. Hare, S. Pothula, R. J. DiLeone, R. S. Duman, *Neuropharmacology* **166**, 107947 (2020).
- S. Deyama et al., *Am. J. Psychiatry* **176**, 388–400 (2019).
- F. Guo et al., *Eur. Neuropsychopharmacol.* **26**, 1087–1098 (2016).

- K. Fukumoto et al., *Neuropsychopharmacology* **45**, 1725–1734 (2020).
- C. Anacker et al., *Nature* **559**, 98–102 (2018).
- B. A. Strange, M. P. Witter, E. S. Lein, E. I. Moser, *Nat. Rev. Neurosci.* **15**, 655–669 (2014).
- A. Burette, U. Zabel, R. J. Weinberg, H. H. W. Schmidt, J. G. Valtchanoff, *J. Neurosci.* **22**, 8961–8970 (2002).
- C. Cserép et al., *Cereb. Cortex* **21**, 2065–2074 (2011).
- G. E. Torres, R. R. Gainetdinov, M. G. Caron, *Nat. Rev. Neurosci.* **4**, 13–25 (2003).
- L. Léger et al., *Histochem. Cell Biol.* **110**, 517–525 (1998).
- K. L. Simpson, B. D. Waterhouse, R. C. Lin, *J. Comp. Neurol.* **466**, 495–512 (2003).
- Q. G. Zhou et al., *J. Clin. Invest.* **129**, 310–323 (2019).
- R. T. Kennedy, *Curr. Opin. Chem. Biol.* **17**, 860–867 (2013).
- Q. G. Zhou et al., *Stem Cell Reports* **9**, 543–556 (2017).

## ACKNOWLEDGMENTS

We thank J. L. Chen., L. D. Li., Y. P. Zhou., M. Y. Zhu., and H. Y. Wu. for assistance with techniques and M. Naveed for editing the revised manuscript. **Funding:** This research was supported by the Brain Research Plan of China (grant 2022ZD0211700) and of Guangdong Province (grant 2018B030334001), the National Natural Science Foundation of China (grants 82071525, 81871065, and 82090042), the Jiangsu Province Natural Science Foundation for Distinguished Young Scientists (grant SBK2019010180), the Key Lab of Cardiovascular and Cerebrovascular Drugs of Jiangsu Province, and the Collaborative Innovation Center for Cardiovascular Disease Translational Medicine for data collection, analysis, and interpretation. **Author contributions:** Q.G.Z., and D.Y.Z. conceived the ideas and prepared the manuscript. T.Y.L. designed the compounds. N.S., Y.J.Q., C.X., T.X., Z.W.D., and L.P.Z. performed experiments and acquired the data. A.-A.L. assisted with in vivo electrophysiology. Y.Z. assisted with cloning. X.L. assisted with measurement of neural transmitters. F.M. and J.Z. supported techniques. D.Y.Z. gave advice for the project and provided part materials for the experiments. **Competing interests:** The authors declare no competing interests. **Data and materials availability:** Plasmids and  $n\text{Nos}^{\text{flox/flox}}$  mice are available upon request from Q.G.Z. (qigangzhou@njmu.edu.cn) under a material transfer agreement with the University of Nanjing Medical University. All data needed to evaluate the conclusions in this study are present in main text or the supplementary materials. **License information:** Copyright © 2022 the authors, some rights reserved; exclusive licensee American Association for the Advancement of Science. No claim to original US government works. <https://www.science.org/about/science-licenses-journal-article-reuse>

## SUPPLEMENTARY MATERIALS

[science.org/doi/10.1126/science.abo3566](https://science.org/doi/10.1126/science.abo3566)

Materials and Methods

Figs. S1 to S10

References (59–73)

MDAR Reproducibility Checklist

[View/request a protocol for this paper from Bio-protocol.](#)

Submitted 28 January 2022; accepted 28 September 2022  
10.1126/science.abo3566

## Design of fast-onset antidepressant by dissociating SERT from nNOS in the DRN

Nan SunYa-Juan QinChu XuTian XiaZi-Wei DuLi-Ping ZhengAn-an LiFan MengYu ZhangJing ZhangXiao LiuTing-You  
LiDong-Ya ZhuQi-Gang Zhou

*Science*, 378 (6618), • DOI: 10.1126/science.abo3566

### A new class of antidepressant drugs

Presently available antidepressant drugs have unpleasant side effects, addictive properties, or can induce schizophrenia. Developing fast-onset antidepressants without these drawbacks is thus an important neuropharmacological goal. Sun *et al.* discovered that dissociating the serotonin transporter from nitric oxide synthase specifically reduced intercellular serotonin concentration in a brain region called the dorsal raphe nucleus. Disrupting this interaction enhanced serotonergic neuron activity in this area and dramatically promoted serotonin release into the medial prefrontal cortex, thereby producing a fast-onset antidepressant effect. A small-molecule blocker of the nitric oxide synthase–serotonin transporter interaction had a fast-onset antidepressant effect in an animal model. —PRS

### View the article online

<https://www.science.org/doi/10.1126/science.abo3566>

### Permissions

<https://www.science.org/help/reprints-and-permissions>

Use of this article is subject to the [Terms of service](#)

---

*Science* (ISSN ) is published by the American Association for the Advancement of Science. 1200 New York Avenue NW, Washington, DC 20005. The title *Science* is a registered trademark of AAAS.

Copyright © 2022 The Authors, some rights reserved; exclusive licensee American Association for the Advancement of Science. No claim to original U.S. Government Works